Proceedings of the XVII ECSMGE-2019
Geotechnical Engineering foundation of the future
ISBN 978-9935-9436-1-3

doi: 10.32075/17ECSMGE-2019-0474

XVII European Conference
ECSMGE 2019
Reykjavik
on Soil Mechanics
and Geotechnical Engineering

The influence of thrust faulting on deep-seated slope gravitational deformation in southern Taiwan

L'influence des failles chevauchement sur les déformations gravitaires profondes de versant au sud de Taiwan

R. F. Chen
Chinese Culture University, Taipei, Taiwan, roufei@earth.sinica.edu.tw

C.W. Lin
National Cheng Kung University, Tainan, Taiwan, chingwee@mail.ncku.edu.tw

H. H. Lin, Y.C. Hsieh,
Central Geological Survey, MOEA, Taipei, linch@moeacgs.gov.tw

C.L. Wang, K.P. Cheng
Soil and Water Conservation Bureau, Nantou, Taiwan

T.C. Chen
National Pingtung University of Science and Technology, Pingtung, Taiwan

ABSTRACT: Meilong River catchment has been chosen to illustrate the influence of thrust faulting on deep-seated slope gravitational deformation in southern Taiwan. We identified morpho-tectonic features using the 1 m resolution LiDAR derived DEM, aerial photographs and field observations. In the 5.2 km^2 catchment, over 10 deep-seated landslides sized over 10 ha have been recognized. Furthermore, a 700 m to 800 m thick faulted material composed of gouge, breccia and intensively fractured metamorphosed metamorphised argillite with thin bedded sandstone was found. Drilling cores from five boreholes with a depth of 120 m to 140 m also support the results of field observations. Fault slip data measured in the field exhibit thrust-type movement that can be used to differentiate faulted material from tectonic origin rather than from gravitation sliding. Besides, as the sliding behavior of identified deep-seated landslides is much more similar to homogeneous cohesive soil than rocks, most of deep-seated landslides observed in the catchments exhibits rotational sliding behavior, which is different from the plane or wedge sliding behavior in most rock slopes in mountainous region of Taiwan.

RÉSUMÉ: Le bassin versant de la rivière Meilong, dans le sud de Taïwan, a été choisi pour illustrer l'influence des failles chevauchement sur les déformations gravitaires profondes de versant. Dans le bassin versant, couvrant une superficie de 5.2 km^2, nous avons recensés plus de 10 glissements de terrain profonds d'une taille supérieure à 10 ha. Leurs caractéristiques morpho-tectoniques ont été identifié à partir du MNT construit sur la base du LiDAR à 1m de résolution, des photographies aériennes et des observations de terrain. De plus, nous avons identifié une zone faillée large de 700-800m composée de gouges, de brèches et d'une alternance de lits fins de grès et d'argilites métamorphiques intensément fracturées. Les observation sur le terrain sont corroborées par l'analyse de carottes provenant de cinq forages d'une profondeur de 120 m à 140 m. Les données de glissement des failles mesurées sur le terrain montrent un mouvement de type chevauchement (compressif) qui peut être utilisé pour différencier le matériel déformé d'origine tectonique de celui issu de glissement gravitaire. De plus, le comportement mécanique des glissements de terrain profonds se rapprochent plus de celui d'un sol homogène

cohésif que de celui d'une roche. Ainsi, la plupart des glissements de terrain profonds observés le long des bassins versants présentent un mouvement de glissement rotationnel, ce qui les différencie du comportement de glissement plan ou en-coin observés dans la plupart des pentes rocheuses des régions montagneuses de Taiwan.

Keywords: deep-seated landslide, thrust faulting, fault gouge, structure fractures

1 INTRODUCTION

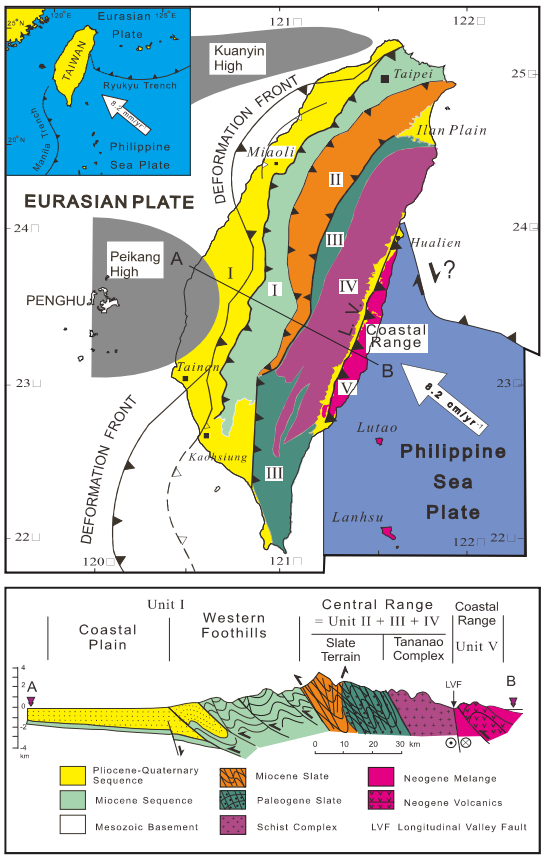

Figure 1. The geodynamic relationships of Taiwan indicate the major tectono-stratigraphic units (Teng, 1990).

Taiwan is located between the Philippine Sea plate and Eurasian plate, with two opposite-verging subduction system of the Ryukyu arc-trench and Luzon arcs to the east and south respectively. Figure 1 indicates the major tectono-stratigraphic units of Taiwan from the east to west (Ho et al., 1986), including the Coastal Range (V); metamorphic Basement (IV); Backbone Rang (III); Hsuehshan Range (II); Western Foothills (Ia) and Coastal Plain (Ib). During tectonic deformation, intensively fractured and pulverized rocks are commonly associated with the development of thrust-faulting on a regional scale.

Fault damage zone is favorable for slow-moving landslides due to reduced bulk-rock strength and contribute to dismantle active mountain belts faults. Therefore, the distributed locations of deep-seated landslides are often highly correlated to the location of regional geological structure (Burbank et al., 1996; Larsen et al., 2010; Scheingross et al., 2013; Guzzetti et al., 2016). Taiwan lies in the path of severe tropical cyclones known in East Asia as typhoons. With their violent wind and extremely heavy rainfall, these storms often cause severe damages. Besides, topographic changes are important even within a relatively short period because earthquakes and typhoons can affect erosion in the case of Taiwan.

The 2009 Typhoon Morakot event induced over 20,000 landslides in souther Taiwan and some fault outcrops along the Meilong River were therefore exposeed, enabling us to better understand the relationship between the active orogenic belt and landscape evolution of Taiwan. Due to limited accuracy and resolution of terrain data, topographic evidence for normal faulting was not clearly identified or found at the time. With the progress of surveying technology, meter-scaled geomorphic features can be displayed and analytically studied using high-resolution digital elevation models (DEMs). In

this study, field investigation and geomorphic analysis were carried out using LiDAR derived DEMs to explore the features of gravitational slope deformation in mountainous region of Taiwan.

In this study, an area of about 25 km^2 at Chulin in southwestern Taiwan was selected to illustrate the importance of geological structure and faulted material on the development of deep-seated landslides. Field observations and interpretations of 1 m resolution LiDAR derived DEM were carried out to clarify the structural, geological and geomorphological setting in which the deep-seated landslide was developed.

2 STUDY AREA

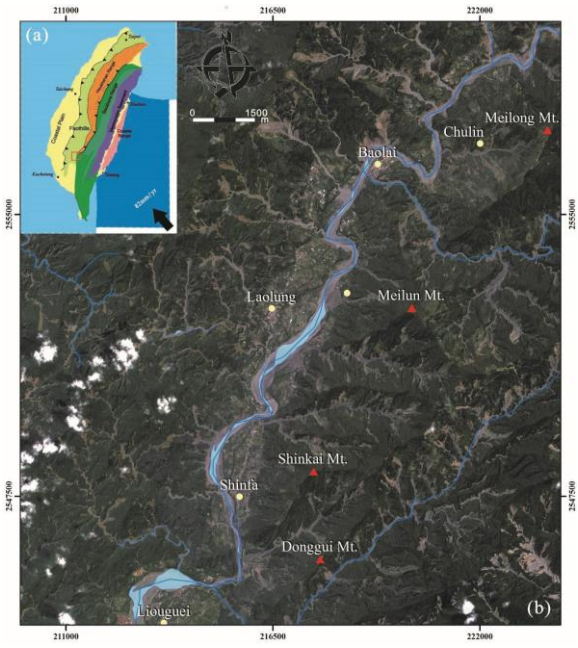

Figure 2. (a) Bathymetric and tectonic framework around Taiwan. (b) Orthoimage of Formosat-2 satellite, showing severe landslides that occurred during the 2009 Typhoon Morakot in the study area.

Chulin, a region of about 25.2 km2 in Paolai District of Kaohsiung City in southwestern Taiwan, was selected as the study area. Within the study area, we mainly focused on the Meilong River catchment due to its better exposures in fault outcrops (Figure 2). Meilong River is an east-to-west flowing small river with a total length of about 2800 m. The Meilong River catchment is about 5.62 km2 and elevation of its catchment is from 430 m to 1350 m.

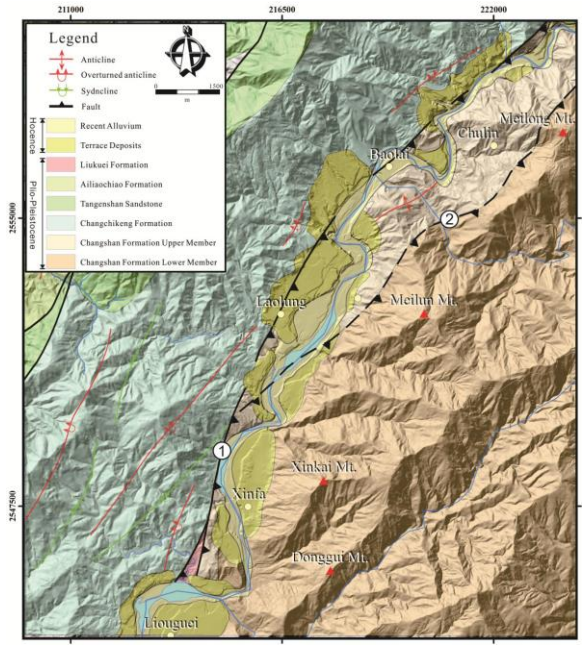

Figure 3. Geological map of the study area (modified by Sung et al., 2000) .

The study area is nearby the intersection of two geological provinces, Western Foothills in the west and Central Mountain Range in the east. The fault contact between Western Foothills and southern Taiwan is Laonung River Fault. There are two faults, the Laonung River Fault that passes through the northern corner and the Meilongshan fault passes through the center of study area (Sung et al., 2000). The Laonung River Fault is an eastern dipping high-angle reverse fault that separates the Miocene sedimentary Changchikeng Formation in the west and the Miocene metamorphosed Changshan Formation in the east. The Changchikeng Formation is primarily composed of grey to dark grey shale with thin bedded sandstone or interbedded thin

layer of shale and sandstone, and the Changshan Formation mainly consists of argillite or slate with thin bedded metamorphosed sandstone. The Meilongshan Fault is an inferred fault because no outcrop had been discovered in precedent field surveys (Figure 3).

3 DATASETS AND STUDY METHODS

The dataset that we used to interpret geomorphic features of deep-seated landslides, including 1 m resolution LiDAR DEM and 25 cm resolution digital aerial photographs, both were from Central Geological Survey (CGS). The LiDAR data was acquired from Leica ALS60/DMC equipped on an airplane flying around 4,000 m with a pulse rate of 44.3 kHz. The digital aerial photographs have elementary position information derived from the on board IMU, and have been orthorectified with the LiDAR derived DEM data on the same flight. The average survey point density for LiDAR was specified to be greater than 2 points/m^2 to generate 1 m resolution DEM.

We manually analyzed the landslide signatures using the LiDAR derived DEM and aerial photographs. Grayscale images of slope inclinations derived from DEM, which are proven to be effective in identifying geomorphic features of deep-seated landslides than the surrounding slopes (Agliardi et al., 2001; Chigira et al., 2013; Chen et al., 2015), were employed to identify landslide morphologic features such as main escarpment, double ridge, trench, reverse slope, crown scarp, extension fracture, transverse ridge and crack, and deformed slope toe; 3D viewed images by Arc sense of Arc GIS were also used to identify abovementioned features; aerial photos with 25 cm resolution were used to identify the geomorphic features of deep-seated landsides, current occurring landslides, and talus or debris deposits. In the field observations of deep-seated landslides, the main investigation items are gully, scarp, multiple ridge and trench, as they can help us to delimit deep-seated landslides. Besides, by investigating the cracks, damages of building and existing shallow landslides, and activity of the sliding mass of deep-seated landslide can also be determined.

4 RESULTS

Within the Meilong River catchment, thirteen deep-seated landslides, which are over 10 ha respectively and about 3.78 km2 in total, were identified within the study area of 5.2 km^2. Five deep-seated landslides with an area less than 10 ha respecively and 0.17 km^2 in total were also discerned. Additionally, 57 shallow landslides with a total area of 122.5 ha were also recognized. One deep-seated landslide was selected to elaborate the details of its morpho-tectonic features recognized in LiDAR derived DEM (Figure 4).

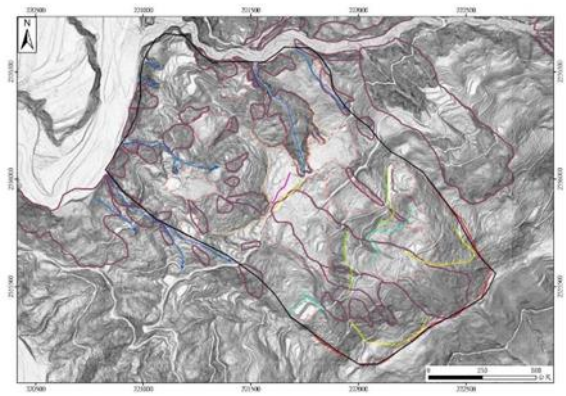

Figure 4. The identified deep seated landslides with an area over 10 ha and less than 10 ha are marked by black and purple line, respectively. The identified shallow landslides are marked by blue lines.

Sized around 150 ha, the site is 870 m wide and 1,600 m long, and has an average slope gradient of 29° and elevation difference of 660 m. Within the deep-seated landslide, 33 shallow landslides with total area of 44 ha can be easily discerned by vegetation stripped off in aerial photos. The main escarpment of this deep-seated landslide is on the ridge and extended about 700 m with a maximum scarp height of about 20 m. A multiple ridge with

a meter depression extended about 200 m was also recognized in middle of the slope. Two main gentle slopes previously covered by landslide deposits were also identified at the height of 890 m and 700 m respectively (Figure 5).

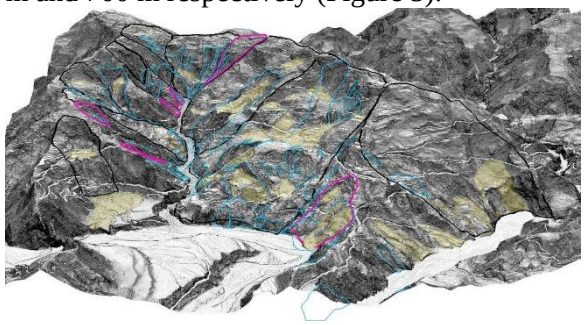

Figure 5. 3D view of identified deep seated landslides and shallow landslides in the study area.

Within the Meilong River watershed, outside of the fault zone, all mapping units exhibit their attitudes fall within the range of N50ºE-N80ºE in strike, and with a dip angle of over 66º toward the east. However, the attitudes of bedding become chaos in the fault zone. Due to high weathering of argillites and debris slide deposit that has covered many areas, only few outcrops can be investigated except along the Meilong River basin. The core of deformed Meilungshan Fault was observed at Outcrop located on the left bank of the Meilong River.

In this study, a fault zone is divided into fault gouge zone, intensively fracture and fault breccia zone, fracture zone, and undeform wall rocks. Fault gouge consists of very fine crushed materials that are generally over 70% in volume and it usually appears in the field as a narrow dark color belt; fault breccia zone contains more crushed rock debris and its very fine materials are less than 70%; the intensively fractured zone is formed by intensively fractured rocks.

Although this makes it difficult to to differentiate the bedding and original rock body, we have managed to recognized the area‘s original lithology. In fracture zone, the fractured rocks and the attitude of bedding and fractures can be recognized and are measurable in the field. Wall rocks that represent the undeform rocks also contain a few fractures sometimes.

Figure 6. Field observation of faulted material in the study area.

In Figure 6, a 50 cm thick fault gouge exposed in areas between the yellow lines, and fault breccia zone was identified in an area below the lower yellow line. Area between the yellow and red lines is a 30 m thick fault breccia zone, whereas area above the red line was recognized as highly-fracture zone.

5 DISCUSSIONS

The slope gradient map produced from the 1 m high-precision LiDAR derived DEM clearly shows features of scarp and gully with details. Apart from areas that cannot be reached, over 85% of scarps interpreted from DEM were verified in field surveys, indicating a high accuracy of the interpretation of scarp using the slope gradient map. Nevertheless, interpretation of LiDAR DEM cannot exactly provide all the information about the activity of scarp. Similarly, toe deformation, trench and internal cracks of slide mass are relatively difficult to be interpreted relying on DEM data only. Therefore, field survey is still necessary for a detailed investigation.

The Meilungshan Fault has been mentioned as an inferred fault according to the variation of strata attitude, but there was no evidence

supporting the inference that the fault passed through the study area in previous studies. The field investigation resutls of this study, however, revealed that there were several outcrops in the fault deformation zone of Meilong River basin, and that there was a 700 m to 800 m thick fault deformation zone containing at least 5 gouge zones on the slope of the south bank of Meilong River. While fault gouge zones are low-permeability layers, the fracture zone and highly-fracture zone are ideal for water reservior. Therefore, when the water gathered in fracture and highly-fracture zones are blocked by fault gouge zone, the pore pressure of rock mass gradually increases (such as the seepage discovered in the field survey), resulting in the slip of rock mass.

Together with the field survey data and gentle slope landform of the south bank of Meilong River, it is known that the formation of concave shape slope (collapses in the preceding period) happened in highly-fracture zone. Besides, seepage was frequently found at the intersection of highly-fracture zone and fault gouge. This not only demonstrates conditions described above, but also proves that the water-resistant and catchment characteristics of fault cores and fracture zones have facilitated the formation of regional collapses.

6 CONCLUSIONS

According to the results of this study, the main controlling factor for the development of deep-seated landslide in the Meilong River watershed is the existence of the Meilungshan Fault. The thrusting movement of fault will favor the creation of great topography and is important for the occurance of deep seated gravitational slope deformation (DSGSD). Through decreasing mechanical rock strength due to the development of gouge, breccia and intensively fractured rock mass and thus also increasing susceptibility toward hillslope failure. In the study area, field evidence shows fractures within rock mass as conduits for groundwater and rain flow, and they usually help the rapid delivery of rain water to the sliding plane. This has been suggested as a mechanism to increase pore-water pressure resulting in slope movement. Additionally, as sliding behavior of identified deep-seated landslides is much more similar to homogeneous cohesive soil than rocks due to faulting process, most of deep-seated landslides observed in the catchments exhibits rotational sliding behavior, which is different from the plane or wedge sliding behavior in most rock slopes in mountainous region of Taiwan.

7 ACKNOWLEDGEMENTS

This work is funded by the Central Geological Survey and Soil and Water Conservation Bureau, “Surface displacement observation and deformation analysis in deep-seated landslide areas using InSAR interferometry ” 107 -10.10.2-S2 and “Installed Surface Displacement Monitoing System and the Analysis of Recoding GPS Data for Large Scale Landslide in 2018 ”.

8 REFERENCES

Agliardia, F., Crosta, G., Zanchib, A., 2001, Structural constraints on deep-seated slope deformation kinematics. *Eng. Geol.*, **59**, 83–102.

Bucci F., Santangelo M., Cardinali M., Fiorucci F., Guzzetti F., 2016, Landslide distribution and size in response to Quaternary fault activity: the Peloritani Range, NE Sicily, Italy. *Earth Surface Processes and Landforms*, **41**, 711-720.

Burbank DW, Leland J, Fielding EJ, Anderson RS, Brozovic N, Reid MR, Duncan C., 1996, Bedrock incision, rock uplift and threshold hillslopes in the northwestern Himalayas. *Nature*, **379**, 505–10.

Cadoppi, P., Giardino, M., Perrone, G., Tallone, S., 2007, Litho-structural control, morphotectonics, and deep-seated

gravitational deformations in the evolution of Alpine relief: A case study in the lower Susa Valley (Italian Western Alps), *Quaternary International*, **171–172**, 143–159.

Chen, R. F., Lin, C.W., Chen, Y. H., He, T. C., Fei, L. Y., 2015, Detecting and Characterizing Active Thrust Fault and Deep-Seated Landslides in Dense Forest Areas of Southern Taiwan Using Airborne LiDAR DEM, *Remote Sensing*,**7(11)**, 15443-15466.

Chigira, M.; Tsou, C.Y.; Matsushi, Y., 2013,Topographic precursors and geological structures of deep-seated catastrophic landslides caused by Typhoon Talas. *Geomorphology*, **201**, 479–493.

Ho, C. S. 1986, A synthesis of the geologic evolution of Taiwan. *Tectonophysics*, **125(1-3)**, 1-16.

Larsen I. J, Montgomery D.R., Korup O., 2010, Landslide erosion controlled by hillslope material. *Nature Geoscience*, **3(4)**: 247–51.

Lin, W. 1999, On the laonunghsi fault—A boundary fault between the paleogene and the neogene strata, Southern Taiwan. *Bull. Cent. Geol. Survey*, **12**, 1–24.

Scheingross, J.S., Minchew, B.M., Mackey, B.H., Simons, M., Lamb, M.P., Hensley, S., 2013, Fault-zone controls on the spatial distribution of slow-moving landslides. Geol. Soc. Am. Bull. 125, 473–489.

Sibson, R.H., 1977. Fault rocks and fault mechanisms, *Jour. Of Geol.Soc. London*, **133**, 191-213.

Sung, Q.C.; Lin, C.W.; Lin, W.H.; Lin, W.C., 2000,Chiahsien [Explanatory Text of the Geologic Map of Taiwan 1/50,000]. *Cent. Geol. Survey*, **51**, 26.

Teng, L. S., 1990, Geotectonic evolution of late Cenozoic arc-continent collision in Taiwan. *Tectonophysics*, **183(1-4)**, 57-76.